



Short communication

Optimizing the control of apoptosis by amide/triazole isosteric substitution in a constrained peptoid



Miriam Corredor^a, Jordi Bujons^b, Mar Orzáez^c, Mónica Sancho^c, Enrique Pérez-Payá^{c,d}, Ignacio Alfonso^b, Angel Messeguer^{a,*}

^a Department of Chemical and Biomolecular Nanotechnology, Institute of Advanced Chemistry of Catalonia, IQAC-CSIC, E-08034 Barcelona, Spain

^b Department of Biological Chemistry and Molecular Modelling, Institute of Advanced Chemistry of Catalonia, IQAC-CSIC, E-08034 Barcelona, Spain

^c Laboratory of Peptide and Protein Chemistry, Centro de Investigación Príncipe Felipe, E-46012 Valencia, Spain

^d Instituto de Biomedicina de Valencia, IBV-CSIC, E-46010 Valencia, Spain

ARTICLE INFO

Article history:

Received 15 November 2012

Received in revised form

25 February 2013

Accepted 1 March 2013

Available online 14 March 2013

Keywords:

Apoptosis inhibitors

Triazole

β -lactam

Ugi-4CC

Click chemistry

Molecular docking

ABSTRACT

Apoptosis is a biological process relevant to several human diseases that is strongly regulated through protein–protein complex formation. We have previously reported a peptidomimetic compound as potent apoptotic modulator. Structural studies of this compound showed the presence of *cis/trans* isomers of the exocyclic tertiary amide bond in slow exchange. This information encouraged us to perform an isosteric replacement of the amide bond by a 1,2,3-triazole moiety, where different substitution patterns would mimic different amide rotamers. The syntheses of these restricted analogs have been carried out using the Ugi multicomponent reaction followed by an intramolecular cyclization. Unexpectedly, for one of the proposed structures, a novel β -lactam compound was formed. All compounds showed to efficiently inhibit apoptosis, *in vitro* and in cellular extracts, with slight differences for the corresponding regioisomers. We propose the binding to Apaf-1 as the inhibition mechanism.

© 2013 Elsevier Masson SAS. All rights reserved.

1. Introduction

Apoptosis is a highly regulated cellular pathway responsible for programmed cell death to remove DNA damaged, virally infected, or otherwise unneeded cells. Diverse apoptotic stimuli, including activation of cell surface death receptors, anti-cancer agents, irradiation, lack of survival factors, and ischemia, induce signaling cascades that activate the caspase family of cysteine aspartyl proteases. These caspases are essential to the apoptotic process, as they are required for the initiation and execution of programmed cell death. Effector caspases (e.g., caspases-3 and -7) are responsible for the disassembly of cellular components, while initiator caspases (e.g., caspases-8, -9 and -10) are responsible for the activation of effector caspases. In particular, caspase-9 is activated upon the release to the cytosol of proapoptotic proteins from the

mitochondrial intermembrane space into the cytosol when apoptosis-inducing signals are perceived by the cell [1]. The formation of the apoptosome is a key event in the intrinsic apoptosis pathway. The apoptosome is a holoenzyme multiprotein complex formed by cytochrome *c*-activated Apaf-1, dATP, and procaspase-9. When cytochrome *c* is released from the mitochondria it binds to Apaf-1, triggering a conformational change and the hydrolysis of the Apaf-1 bound dATP/ATP. In a process dependent on the hydrolysis of ATP or dATP to ADP or dADP respectively, the Apaf-1-cytochrome *c* heterodimers assemble into the apoptosome, which provides a platform for the activation of the initiator procaspase-9. Then, the activated caspase-9 cleaves and activates executioner caspases such as caspase-3 [2,3].

Defects in the regulation of apoptosis are related to diseases. The development of new anti-cancer therapies importantly relies on inducing apoptosis. In contrast, tissue infarction, ischemia–reperfusion damage, degenerative diseases, and AIDS showed in common excessive apoptosis-mediated unwanted cell death. To identify molecules that could ameliorate disease-associated excessive apoptosis, drug discovery efforts were directed toward the inhibition of caspase activity, particularly the effector caspase-3 [4]. However, caspase-3 inhibitors have encountered problems in

Abbreviations: Ugi-4CC, Ugi four-component coupling reaction; CuAAC, copper(I)-catalyzed azide–alkyne cycloaddition reaction; RuAAC, ruthenium-catalyzed azide–alkyne cycloaddition reaction; IBX, 2-iodoxybenzoic acid; DKP, 2,5-diketopiperazine.

* Corresponding author. Tel.: +34 400 61 00x2186.

E-mail address: angel.messeguer@iqac.csic.es (A. Messeguer).

their pharmacological development [5]. Alternatively, protein–protein interactions upstream of caspase activation can also be relevant points of intervention for the development of modulators of apoptosis pathways. In particular, recent data propose the formation of the apoptosome as an interesting target for the development of apoptotic modulators.

Understanding the mechanism of functional activation of the apoptosome has helped to define prospective targets for treating deregulated apoptosis associated with human pathologies. One of these targets is the Apaf-1 protein. Our group has developed an efficient *in vitro* and *ex-vivo* methodology for detecting activity of molecules inhibiting the apoptosome formation [4]. Within this project, we identified some active compounds after screening of a diversity-oriented chemical library of *N*-alkylglycine oligomers [4]. Then, geometrical restrictions were devised to increase the selectivity [2] by reducing the conformational freedom. A *hit* compound (**1**) was obtained [6], and structural studies of **1** showed the presence of *cis/trans* isomers of the tertiary amide bond exchanging at slow rates (Fig. 1) [7]. The occurrence of these *cis/trans* isomers has led us to freeze the *cis* and *trans* configuration by isosteric substitution using a triazole moiety [8]. 1,2,3-Triazoles offer an appealing motif in peptidomimetic research [9,10] because their structural and electronic characteristics are similar to those of a peptide bond and general methods are now available for their synthesis [11–13]. In this regard, we hypothesized that the 1,4- and 1,5-disubstituted triazole moieties could mimic the spatial disposition of the residues for the *cis* and *trans* configuration of **1**, respectively (Fig. 1, **2a** and **2b**). As an intermediate situation, we also envisioned the preparation of the 2,4-disubstituted triazole derivative (**2c**).

2. Chemistry

For the syntheses of **2a–c**, we planned a common strategy (Scheme 1) based on an Ugi four-component coupling reaction (Ugi-4CC) [14–17] comprising a primary amine **4**, an aldehyde **5**, an isocyanide **6** and a carboxylic acid **7**, which are condensed to yield a single product (**3**). After the formation of the open products, a base-promoted intramolecular cyclization would yield the final compounds. Most of the corresponding starting materials are commercially available (**4** and **7**) or easily accessible (**6**) by simple

synthetic procedures (see Supplementary data). However, the key triazole aldehydes bearing different substitution patterns (**5a–c**) had to be synthesized through modifications of synthetic methods described in the literature (Scheme 2).

The Cu(I)-catalyzed azide–alkyne cycloaddition (CuAAC), perhaps the most powerful click reaction providing 1,4-disubstituted 1,2,3-triazoles [18,19] has quickly found many applications in synthetic and medicinal chemistry [20,21], bioconjugations [22,23], materials science [24], and polymer chemistry [25]. The success of the CuAAC highlights the need for selective access to the complementary regioisomers. However, 1,5-isomers have been only scarcely explored so far [26,27], although Fokin and coworkers [28,29] recently reported that their preparation can be accomplished by a ruthenium-catalyzed azide–alkyne cycloaddition reaction (RuAAC). This reaction furnishes the triazole derivatives with a virtually total 1,5-regioselectivity [30]. Considering these two complementary catalysts, we envisioned the synthesis of both triazole isomers from the common pair of alkyne (propargyl alcohol) and azide **8**. This approach would render the corresponding alcohols, which can be easily transformed into the aldehydes **5a,b** by mild oxidation with IBX (Scheme 2). Thus, the 1,4-disubstituted-1,2,3-triazole was formed using CuSO₄/ascorbic acid in water/THF. For the case of the 1,5-disubstituted 1,2,3-triazole, the Cp*RuCl(PPh₃)₂ catalyst was used, showing to be less efficient and selective than the CuAAC process. In addition to the low conversion (40%) of the Ru-catalyzed reaction, the yield was additionally hampered by the exhaustive chromatographic separations necessary to obtain pure material.

On the other hand, the 2-substituted-2*H*-1,2,3-triazoles can be obtained by alkylation of *NH*-1,2,3-triazoles with the suitable electrophilic reagents, although a mixture of the isomeric products is often produced. A general and simple method for the synthesis of the 2*H*-isomers is not still available. In 2008, Fokin and coworkers reported an elegant three-component one-pot synthesis of 2-hydroxymethyl-2*H*-1,2,3-triazoles [31]. These compounds are versatile intermediates that can be used for the preparation of *NH*-1,2,3-triazoles. In their method, formaldehyde, sodium azide and a terminal alkyne (propargyl alcohol in our case) react in a one-pot two-steps process under acid conditions. A mixture of the 1-hydroxymethyl-1,2,3-triazole and the 2-hydroxymethyl isomer was obtained, being the desired isomer the major and the most stable one. Basic hydrolysis of the *N*-hydroxymethylalcohol led to the parent *NH*-compound (Scheme 2B). Finally, a simple S_N2 reaction at N-2 of the triazole with the corresponding bromide afforded the 4-hydroxymethyl-2,4-disubstituted-triazole derivative, which was also transformed into the corresponding aldehyde (**5c**) by oxidation with IBX (Scheme 2). The substitution patterns of the three isomeric triazoles were unambiguously established by a complete NMR assignment of the signals of **5a–c** and those of their corresponding alcohol precursors, including the ¹⁵N NMR signals from ¹H–¹⁵N gHMBC 2D experiments (see Supplementary data).

Once all the reagents of the Ugi-4CC reaction were available, the final products could be synthesized. The Ugi reaction requires a high concentration in the mixture and a specific order of addition. Considering that the formation of the imine is a key step for the progress of the overall reaction, it was monitored by ¹H NMR. We concluded that the imine was formed in 6 h; afterward, the addition of the isocyanide and the carboxylic acid must be done within 30 min. The addition of the acid before this period of time produced the hydrolysis of the imine and prevented the formation of the Ugi products. To afford the final DKP products from **3a–c**, two different basic treatments were used due to the different reactivity of the structures. For **3a**, a KOH/MeOH mixture was used and the desired product **2a** was formed; but when the same method was used for **3b**, the hydrolyzed product was obtained. Then, a NaH/THF system

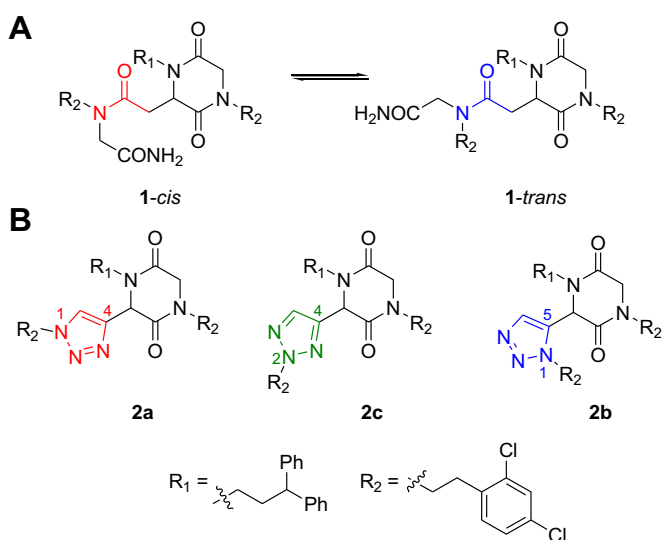
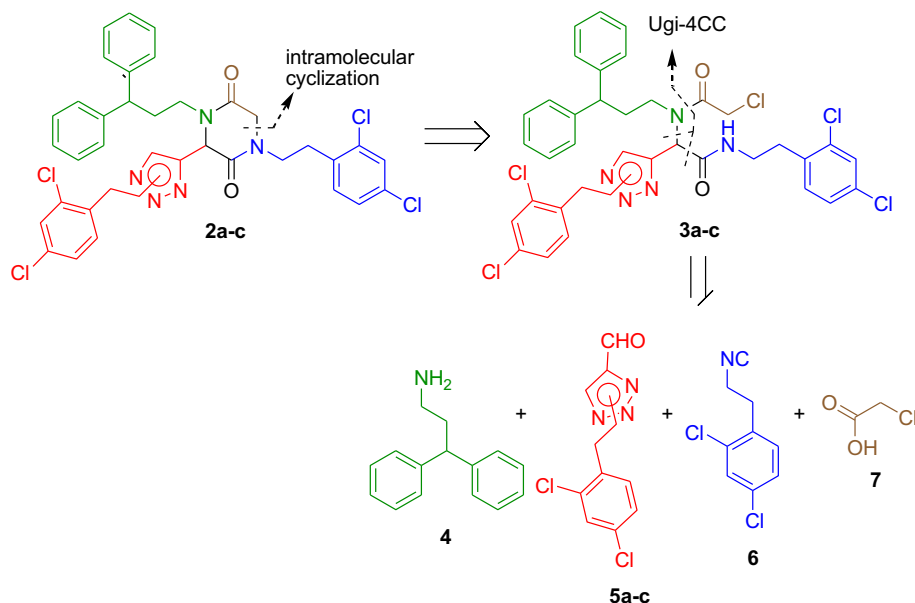


Fig. 1. A) Structure of apoptosis inhibitor **1**. B) Proposed conformationally restricted analogs bearing the 1,2,3-triazole residue.



Scheme 1. Retrosynthesis of **2a–c** comprising an Ugi-4CC reaction followed by an intramolecular cyclization.

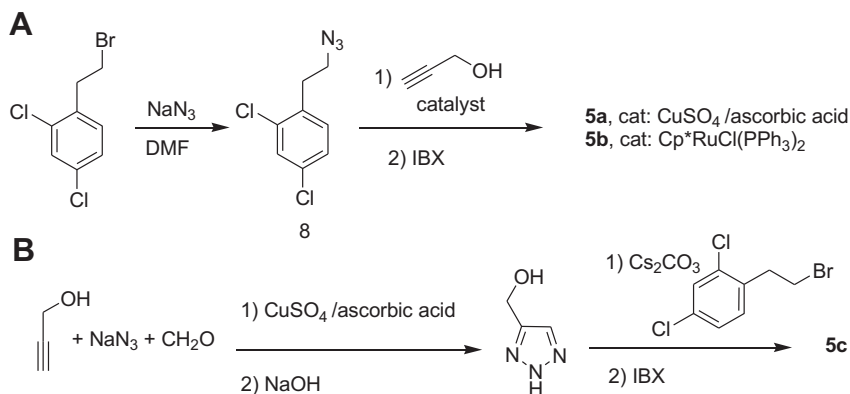
was assayed and the cyclic compound **2b** was isolated after preparative TLC purification. Noticeably, when using any of these methods with **3c**, an unexpected product was formed. This compound had the same mass of **2c** in the ESI-MS spectrum ($m/z = 720.14$ for MH^+), but the 1H NMR spectrum showed an amide NH signal that should disappear when forming the DKP, while the CH of the chiral center of the DKP was absent, suggesting that the intramolecular cyclization had occurred through the corresponding carbon atom. After carefully analyzing the NOESY, 1H – ^{13}C gHSQC/gHMBC, and 1H – ^{15}N gHMBC NMR spectra, as well as the FT-IR spectrum, the proposed structure **9** was confirmed (Fig. 2). We also included compound **9** in the biological assays as apoptosis inhibitors.

3. Biological activity and docking studies

All the compounds (**1**, **2a,b** and **9**) were potent *in vitro* inhibitors of the apoptosome-dependent activation of procaspase-9 activity (Fig. 3 and Supplementary data). Moreover, none of them was a direct inhibitor of the activity of recombinant caspase-9, which suggests that the most probable target is apoptosome formation. As

shown in Fig. 3, an improvement of the activity was obtained in the triazole compounds, with slight differences for the two regioisomers **2a,b**. It is also worth mentioning that the β -lactam structure **9** elicited the best activity. Similar inhibitory trends were observed in cellular extracts (Supplementary data). This is an interesting starting point to further study this new scaffold in the design of optimized apoptosis inhibitors. In addition, these results support our initial hypothesis that a more rigid structure could favor the interaction with the target protein. On the other hand, we deem that the more restricted conformational freedom of these compounds will reduce the risks associated to interaction with non-desired targets.

A preliminary blind docking screening for a related 7-membered cyclic analog of **1** targeting the reported human Apaf-1 1-591 structure [32], revealed potential binding sites at the CARD–NOD interface (Site 1) and at the reported ADP binding site in the NOD domain (Site 2). These two predicted binding sites on Apaf-1 were consistent with experimental results that demonstrated the interaction between this analog and Apaf-1 [33]. Interestingly, in the crystal structure these binding sites are connected through a narrow channel (Fig. 4A), which constitutes the only apparent entrance



Scheme 2. Syntheses of aldehydes **5a–c**.

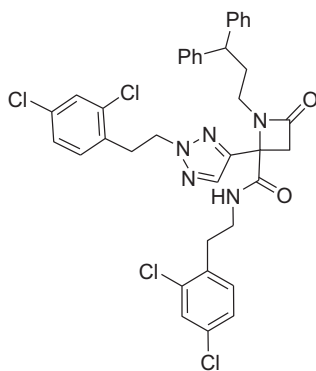


Fig. 2. Compound 9.

to the deeply buried nucleotide binding site (NBS), suggesting that access to this site requires unpacking of the CARD–NOD interface [32]. Thus, inhibitor binding at Site 1 could obstruct the access of dATP to the NBS by blocking the entrance to this channel and, possibly, by stabilizing Apaf-1 into a “locked” conformation that would hinder unpacking of the CARD–NOD interface. Alternatively, binding at Site 2 would directly block the NBS. Therefore, interaction with any of these sites, or both, would hamper dATP binding, and consequently would interfere with apoptosome formation.

Those docking studies have now been extended to compounds **1**, **2a**, **2b** and **9**. Since all of these compounds have a single stereogenic center on their structures, independent docking runs were carried out for each enantiomer. Fig. 4B–D shows the best poses obtained for compound (*R*)-**9** at each of the two putative binding sites.

Site 1 is located on a large cleft at the CARD–NOD interface and it is formed by helices $\alpha 2$, $\alpha 3$, $\alpha 5$, $\alpha 7$, $\alpha 8$, and the loop between residues 117 and 129. According to our docking results, at Site 1 compound (*R*)-**9** is disposed along this cleft covering the entrance to the NBS access channel, with its diphenylmethyl moiety occupying a cavity formed by residues His28, Asp32, His77, Lys100, Arg111, and Arg122 (Fig. 4B,C). The two aromatic rings of this moiety establish π -cation and π,π -stacking interactions with residues Lys100 and His77, respectively. All the other compounds similarly showed occupation of this cavity by their diphenylmethyl or one of their dichlorophenyl moieties, which were also stabilized by similar interactions with the cited residues (see Supplementary data for details). On the other hand, one of the dichlorophenyl substituents of (*R*)-**9** extends to the other side of the cleft and forms a π -cation interaction with residue Arg332, while the second dichlorophenyl group is oriented toward the more solvent exposed

part and is disposed on top of a small hydrophobic patch on the surface of the protein, formed by residues Val125 and Leu297. Finally, the exocyclic amide and the carbonyl group of the β -lactam ring contribute to stabilize the docked pose of (*R*)-**9** by participating on hydrogen-bond interactions with residues Val124 and Arg428. Analysis of the docking poses obtained for the enantiomeric (*S*)-**9** and the rest of the compounds studied showed similar results (see Supplementary data). Hence, a common feature of the compounds bound at Site 1 was the formation of several π -cation interactions with different cationic residues (i.e. Lys100, Arg111, Arg122 and Arg332), as well as hydrogen bond interactions with the polar side-chains or the backbone of close residues, while the contribution of hydrophobic interactions at this site was in general less important (see Table S1, Supplementary data).

Concerning the predicted binding Site 2, which as mentioned above coincides with the nucleotide binding site, it is constituted by a relatively large cavity (Fig. 4A) formed by helices $\alpha 10$, $\alpha 15$ and $\alpha 17$, sheets $\beta 2$, $\beta 6$ and $\beta 7$, and loops between residues 117–129, 154–159 and 389–394. The residues that constitute this cavity are mainly hydrophobic in nature, particularly in the region close to the location of the purine ring of the bound ADP (i.e. residues Pro123, Val125, Phe126, Val127, Val162, Ile294 and Pro321). The best docked pose obtained for compound (*R*)-**9** fills most of the cavity and partially overlaps with the crystallographically determined ADP molecule (Fig. 4B,D), suggesting that both compounds would compete for binding at this Site. Its diphenylmethyl moiety occupies the same location as the purine system of ADP, while one of the dichlorophenyl rings is disposed in an approximately parallel orientation, surrounded by residues Pro120, Pro123, Val162 and Ala165, and the second one extends toward a more hydrophilic region of the cavity, constituted by the polar residues Lys160, Asp243, Asp244, Arg265, Asp392, His438 and Asp439. Finally, the triazole ring of (*R*)-**9** occupies the region where the diphosphate group of ADP binds, establishing a π,π -stacking interaction with His438 and a hydrogen bond with the backbone NH-group of Gly159, while the β -lactam is disposed close to the location of the ADP-ribose group. On the other hand, the best docked pose of the stereoisomer (*S*)-**9** shows an inverted geometry where the diphenylmethyl and dichlorophenyl moieties that were occupying the hydrophobic locations described above have switched places, while the second dichlorophenyl ring and the linked triazole still occupy the more hydrophilic region and the diphosphate binding site, respectively (see Supplementary data). The rest of the compounds considered show best docked poses which are similar to that of (*S*)-**9**, with the exception of compound (*S*)-**1** which resembles more to (*R*)-**9** (see Supplementary data). The existence of these alternative docking geometries is derived from the flexibility of the compounds, as well as the large size of the cavity and the fact that the main stabilizing interactions with the protein are of hydrophobic, and therefore less specific, nature.

After analysis of these results, it is worth noting that the relative similarity in bound geometries and binding interactions at each site is in agreement with the comparable biological activities observed for these compounds. It is also remarkable that, considering the best poses obtained for all the compounds, the average docking scores for Sites 1 and 2 are 4.9 ± 1.0 and 8.1 ± 1.7 kcal mol⁻¹. Although docking scores alone often show little correlation with experimental binding affinities, this difference would suggest that binding at Site 2 is stronger than at Site 1. Preliminary prediction of the affinities using more accurate methodologies (i.e. MMGBSA) confirm this suggestion (results not shown). Therefore it could be speculated that Site 1 could act as a vestibule where the compounds studied here could bind with a relatively low affinity before accessing the higher affinity NBS-Site 2 to exert their apoptosome inhibitory activity.

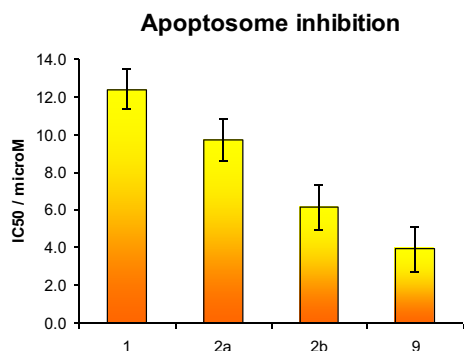


Fig. 3. *In vitro* inhibitory activities on the apoptosome formation by the triazole derivatives **2a**, **2b** and **9**. Activity of DKP **1** is shown for comparative purposes.

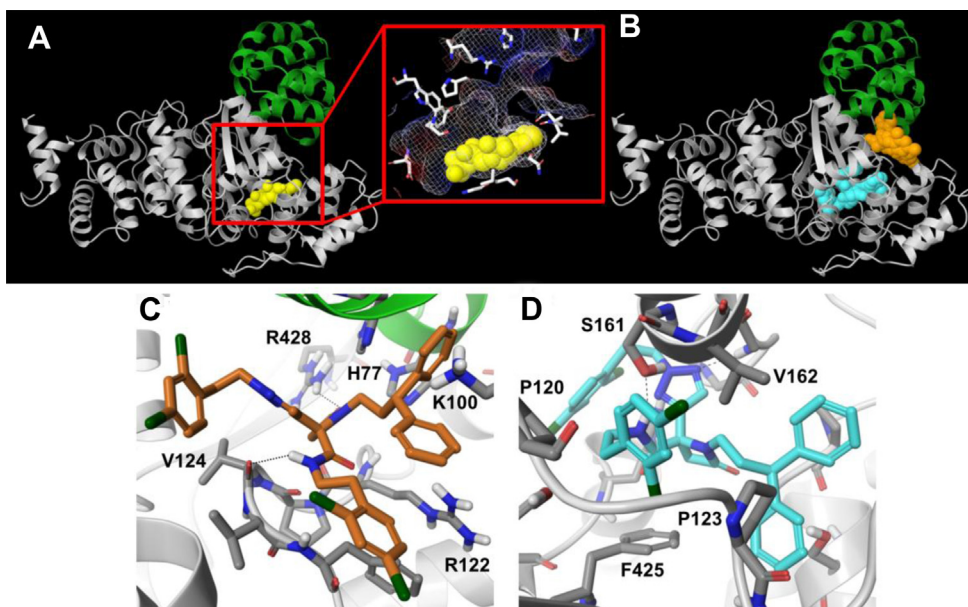


Fig. 4. A) Human Apaf-1 1–591 structure (PDB 1Z6T) showing the CARD (green) and NOD (light gray) domains, as well as a crystallographically determined ADP molecule (yellow) bound into the NBS. The inset shows the bound ADP molecule surrounded by Apaf-1 residues, and a mesh representation of the protein surface that reveals a narrow channel connecting the NBS with the exterior. B) Best docked poses of compound (R)-9 bound at the putative binding sites 1 (orange) and 2 (cyan). C) and D) Detailed view of the above docked poses at the two sites surrounded by interacting Apaf-1 residues (see Supplementary data for detailed interaction diagrams). Docking was performed with the program Glide XP [34–37]. (For interpretation of the references to colour in this figure legend, the reader is referred to the web version of this article.)

4. Conclusions

In conclusion, it has been shown that geometrically restricted analogs of a peptoid derivative by amide/triazole isosteric substitution maintain their activities as apoptosis inhibitors. Moreover, an unexpected and structurally novel β -lactam derivative showed the best activity among all the tested compounds.

Funding sources

This work was supported by grants from the Spanish Ministry of Science and Innovation (SAF2008-00048, SAF30542-C01-01 and SAF2010-15512) and a fellowship to M. Corredor from CSIC JAE program.

Appendix A. Supplementary data

Supplementary data related to this article can be found at <http://dx.doi.org/10.1016/j.ejmech.2013.03.004>.

References

- [1] E. Pérez-Payá, M. Orzáez, L. Mondragón, D. Wolan, J.A. Wells, A. Messeguer, M.J. Vicent, *Med. Res. Rev.* 4 (2011) 649–675.
- [2] L. Mondragon, M. Orzáez, G. Sanclimens, A. Moure, A. Armiñán, P. Sepúlveda, A. Messeguer, M.J. Vicent, E. Pérez-Payá, *J. Med. Chem.* 51 (2008) 521–529.
- [3] E.C. Ledgerwood, I. Morison, *Clin. Cancer Res.* 15 (2009) 420–424.
- [4] G. Malet, A.G. Martín, M. Orzáez, M.J. Vicent, I. Masip, G. Sanclimens, A. Ferrer-Montiel, I. Mingarro, A. Messeguer, H.O. Fearnhead, E. Pérez-Payá, *Cell. Death Differ.* 13 (2006) 1523–1532.
- [5] C.W. Scott, C. Sobotka-Briner, D.E. Wilkins, R.T. Jacobs, J.J. Folmer, W.J. Frazee, R.V. Bhat, S.V. Ghanekar, D. Aharony, *J. Pharmacol. Exp. Ther.* 304 (2003) 433–440.
- [6] A. Moure, M. Orzáez, M. Sancho, A. Messeguer, *Bioorg. Med. Chem. Lett.* (2012) 7097–7099.
- [7] A. Moure, G. Sanclimens, J. Bujons, I. Masip, A. Alvarez-Larena, E. Pérez-Payá, I. Alfonso, A. Messeguer, *Chem. Eur. J.* 17 (2011) 7927–7939.
- [8] M. Tischler, D. Nasu, M. Empting, S. Schmelz, D.W. Heinz, P. Rottmann, H. Kolmar, G. Buntkowsky, D. Tietze, O. Avrutina, *Angew. Chem. Int. Ed.* 51 (2012) 3708–3712.
- [9] W.S. Horne, M.K. Yadav, C.D. Stout, M.R. Ghadiri, *J. Am. Chem. Soc.* 126 (2004) 15366–15367.
- [10] J.M. Ahn, N.A. Boyle, M.T. MacDonald, K.D. Janda, *Mini-rev. Med. Chem.* 2 (2002) 463–473.
- [11] D.J. Pedersen, A. Abell, *Eur. J. Org. Chem.* 13 (2011) 2399–2411.
- [12] P. Wu, V.V. Fokin, *Aldrichimica Acta* 40 (2007) 7–17.
- [13] C.W. Tornøe, C. Christensen, M. Meldal, *J. Org. Chem.* 67 (2002) 3057–3064.
- [14] R. Bossio, C.F. Marcos, S. Marcaccini, R. Pepino, *Tetrahedron Lett.* 38 (1997) 2519–2520.
- [15] S. Marcaccini, R. Pepino, M.C. Pozo, *Tetrahedron Lett.* 42 (2001) 2727–2728.
- [16] M. Mroczkiewicz, R. Ostasqewski, *Tetrahedron* 65 (2009) 4025–4034.
- [17] M.J. Thompson, B.N. Chen, *J. Org. Chem.* 74 (2009) 7084–7093.
- [18] H.C. Kolb, M.G. Finn, K.B. Sharpless, *Angew. Chem. Int. Ed.* 40 (2001) 2004–2021.
- [19] V.V. Rostovtsev, L.G. Green, V.V. Fokin, K.B. Sharpless, *Angew. Chem. Int. Ed.* 41 (2002) 2596–2599.
- [20] C.H. Zhou, Y. Wang, *Curr. Med. Chem.* 19 (2012) 239–280.
- [21] H.C. Kolb, K.B. Sharpless, *Drug Discov. Today* 8 (2003) 1128–1137.
- [22] A.J. Link, D.A. Tirrell, *J. Am. Chem. Soc.* 125 (2003) 11164–11165.
- [23] Q. Wang, T.R. Chan, R. Hilgraf, V.V. Fokin, K.B. Sharpless, M.G. Finn, *J. Am. Chem. Soc.* 125 (2003) 3192–3193.
- [24] C.J. Hawker, V.V. Fokin, M.G. Finn, K.B. Sharpless, *Aust. J. Chem.* 60 (2007) 381–383.
- [25] R.A. Evans, *Aust. J. Chem.* 60 (2007) 384–395.
- [26] A. Tam, U. Arnold, M.B. Soellner, R.T. Raines, *J. Am. Chem. Soc.* 129 (2007) 12670–12671.
- [27] D. Imperio, T. Piralli, U. Galli, F. Pagliai, L. Cafici, P.L. Canonico, G. Sorba, A.A. Genazzani, G.C. Tron, *Bioorg. Med. Chem.* 15 (2007) 6748–6757.
- [28] L. Zhang, X. Chen, P. Xue, H.H.Y. Sun, I.D. Williams, K.B. Sharpless, V.V. Fokin, G. Jia, *J. Am. Chem. Soc.* 127 (2005) 15998–15999.
- [29] B.C. Boren, S. Narayan, L.K. Rasmussen, L. Zhang, H. Zhao, Z. Lin, G. Jia, V.V. Fokin, *J. Am. Chem. Soc.* 130 (2008) 8923–8930.
- [30] R. Mounné, V. Larue, B. Seijo, T. Lecourt, L. Micouin, C. Tisné, *Org. Biomol. Chem.* 8 (2010) 1154–1159.
- [31] J. Kalisiak, K.B. Sharpless, V.V. Fokin, *Org. Lett.* 15 (2008) 3171–3174.
- [32] S.J. Riedl, W. Li, Y. Chao, R. Schwarzenbacher, Y. Shi, *Nature* 434 (2005) 926–933.
- [33] To be published elsewhere.
- [34] Glide, Schrodinger, LCC, New York, NY, 2012.
- [35] R.A. Friesner, J.L. Banks, R.B. Murphy, T.A. Halgren, J.J. Klicic, D.T. Mainz, M.P. Repasky, E.H. Knoll, M. Shelley, J.K. Perry, D.E. Shaw, P. Francis, P.S. Shenkin, *J. Med. Chem.* 47 (2004) 1739–1749.
- [36] T.A. Halgren, R.B. Murphy, R.A. Friesner, H.S. Beard, L. Frye, W.T. Pollard, J.L. Banks, *J. Med. Chem.* 47 (2004) 1750–1759.
- [37] R.A. Friesner, R.B. Murphy, M.P. Repasky, L.L.M. Frye, J.R. Greenwood, T.A. Halgren, P. Sanschagrin, D.T. Mainz, *J. Med. Chem.* 49 (2006) 6177–6196.